Impacts of Complex Terrain on Evapotranspiration within a Tropical Alpine Valley in the Peruvian Andes

R.A. HELLSTRÖM[1], AIMEE HIGGINS[1], DEREK FERRIS[1], BRYAN MARK[2], AND DELPHIS LEVIA[3]

ABSTRACT:

Northern Peru will face critical water resource issues in the near future as permanent ice in the Andes Mountains retreats. Much of current global and regional climate research assumes that evapotranspiration (ET) is a negligible part of the water cycle in the Peruvian Andes due to lack of precipitation during the dry season and high humidity during the wet season. However, recent measurements from an embedded sensor network (ESN) indicate that ET from a typical pro-glacial valley contributes to the Andean water cycle in Peru. In 2005 and 2006, we installed an ESN consisting of discrete, cost-effective automatic temperature and humidity loggers along the valley axis and four automatic weather stations to better understand near-surface boundary layer processes controlling moisture flux from the 39% glacierized Llanganuco Valley, Cordillera Blanca, Peru (9º south). This project incorporated LandSat ETM+ images, temperature profiles from the ESN, NCEP/NCAR reanalysis and evapotranspiration (ET) modeling to demonstrate that ET from non-glacierized land cover depends on the valley's terrain and land cover and it varies according to seasonal and daily time scales. We compared diurnal and seasonal cycles of temperature, moisture and wind patterns from the ESN with NCEP/NCAR upper air data to reveal important intra-valley meteorological processes that could influence ET and glacial mass balance. This research emphasizes the need for better understanding of multi-scale processes in alpine valleys.

Keywords: evapotranspiration, diurnal cycles, tropical, alpine

INTRODUCTION

The Andes Mountains are located in western South America, most notably in the countries of Ecuador, Peru and Chile. Peru (Figure 1) is a nation facing critical water resource issues (Bradley *et al.*, 2006; Mark and Seltzer 2003; Mark and Seltzer 2005; Vergara *et al.*, 2007). There are currently eighteen glaciers that exist in Peru, of which twenty two percent has been lost over the past thirty years (World Bank, 2008). While observations of continued glacier recession exist throughout the Andes, only a few efforts have been made to quantify the relative significance of the fluxes in the regional hydrological cycle. Steep U-shaped valleys carved out by receding glaciers, known as proglacial valleys, often contain moraine-dammed lakes and are the primary drainage conduits for melting glaciers and wet-season rainfall in the Cordillera Blanca; note the

[1]Geography Department, Bridgewater State University, Bridgewater, MA 02325
[2]Department of Geography, The Ohio State University, Columbus, OH 43210
[3]Department of Geography and Center for Climate Research, University of Delaware, Newark, DE 19716

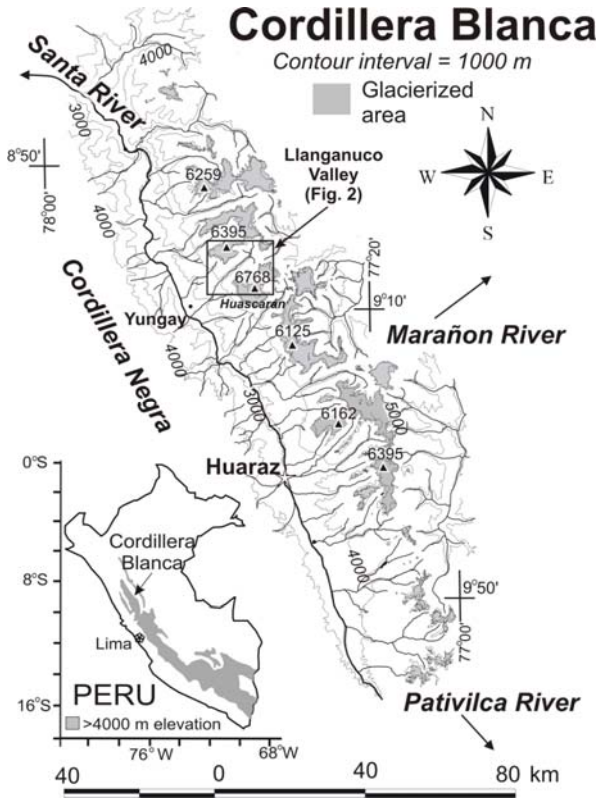

Figure 1. Cordillera Blanca regional map. The Llanganuco Valley is one of several pro-glacial valleys in the region. These valleys supply water to the Santa River running northwest-ward between the Cordillera Negra and Blanca.

south-west trending valleys along the west-facing slope (Figure 1). Previous studies have primarily focused on the rates, controls, and flux of glacier melt water directly from and within the glaciers (Francou et al., 1995; Francou et al., 2003; Juen et al., 2007; Ramirez et al., 2001; Wagnon et al., 1999; Wagnon et al., 1998), or assess the relative contribution of glacier meltwater to streamflow (Kaser et al., 2003; Mark and Seltzer 2003; Mark and Seltzer 2005; Casassa et al., 2009). These studies have elucidated the critical role of seasonal humidity flux in controlling mass balance by feedbacks to the radiation balance and latent heat. Yet a shortage of distributed in-situ measurements has limited understanding of hydroclimatic processes such as evapotranspiration (ET) within pro-glacial valleys. Contrary to the middle latitudes, the seasonal variation in glacier melt strongly depends on moisture-related variables, rather than on air temperature (Juen 2006; Juen et al., 2007). Recent studies suggest that ET from land is equally as important as ocean sources of water vapour in the tropical hydrological cycle (Worden et al., 2007). Konzelmann et al. (1997) demonstrated that ET is a significant contributor to the hydrological cycle in mid-latitude regions, controlled by vegetation and surface terrain and elevation. Data scarceness has precluded explicit inclusion of ET for consideration in the Andean hydrological budget and thus ET is neglected. An oversimplified assumption considers that ET is reduced during arid times by a lack of available moisture, and then counterbalanced by precipitation during the rainy season (Kaser et al., 2003). A better understanding of local boundary layer processes affecting ET helps fill an outstanding need to better characterize the hydrologic processes on the local to regional scale where humans utilize water resources, and where future management decisions must be made.

While ET in tropical pro-glacial valleys is largely unverified and assumed negligible on interannual time scales, there is reason to believe that the influence of soil, vegetation, and local meteorological forcing can have significant impact on ET over diurnal and seasonal scales. The

low barometric pressure at high elevations also promotes ET, and the incident solar radiation, wind, humidity, precipitation and temperature comprise primary regulating components of meteorological forcing that are strongly variable in tropical highlands on seasonal to diurnal time scales. Precipitation, particularly in the northern Andes, has a pronounced diurnal cycle with higher potential in the late afternoon or at night (Dai 2001). Furthermore, the valley wind circulation described by Whiteman (2000) is driven by a combination of spatial variation in the local surface energy fluxes that create pressure gradients and flow channeled from the free atmosphere. Although incoming solar radiation is the primary forcing of surface temperature, because ET affects turbulent heat flux and hence surface temperature, ET plausibly impacts the valley wind. Current ground-based meteorological observations in the Peruvian Andes, such as (Hardy *et al.*,1998; Vuille *et al.*, 2003) do not extend to pro-glacial valleys, so it is necessary to develop and deploy a new measurement network.

It is difficult and labor intensive to measure ET accurately, particularly in remote mountainous regions with steep topography; most measurements require expensive equipment and frequent maintenance (Canqui 1993; Garcia 2001; Paço *et al.*, 2006; Paredes 1995) or satellite remote sensing techniques (Allen 2000; Kite and Droogers 2000) that require site-specific ground truths. The spatial variability of leaf area index and soil water availability makes it impractical to model ET over heterogeneous landscapes using ground-based in situ techniques. Consequently, there are a multitude of methods for estimating ET, most of which require site specific parameters and basic meteorological measurements, and integration of remote sensing (Eichinger and Cooper 2007; Suleiman and Crago 2004). With respect to high elevation sites in South America, such as the Bolivian Altiplano, Garcia *et al.* (2004) found good agreement between measured reference ET using lysimeters and estimated values from the widely used algorithm of the Food and Agriculture Organization (FAO) of the United Nations Penman-Monteith (P-M) equation (FAO-56 P-M) as described by Allen (2000).

PHYSIOGRAPHY OF THE LLANGANUCO VALLEY, PERU

The Andean Cordillera Blanca is home to the greatest concentration of tropical glaciers on earth (Figure 1). It is the largest and most northerly mountain range in Peru, trending northwest-southeast over 130 km between 8°10° south latitude (Ames 1998) along the Andean continental divide. Most of the glacierized area in the Cordillera Blanca discharges northwest via the Santa River, that has the least variable monthly runoff of all Pacific draining rivers. Andean climate is semi-arid in the valleys and moist in higher elevations with a distinct rainy season between October and April and dry the remaining months.

The Llanganuco Valley is a U-shaped hanging valley tributary draining southwest to the Santa River (Figure 2). Its mouth is flanked by steep walls of the glacially sculpted granodiorite bedrock that comprises the Upper Miocene batholithic core of the range (McNulty et al., 1998). Summits that border the catchment include Huascarán at 6,768 meters above mean sea-level (m a.s.l.) to the south, highest in Peru, the Huandoy massif (6,395 m a.s.l.) to the north, and Chacraraju (6,113 m a.s.l.) to the east. The Valley contains two lakes, and is a well-visited tourist attraction within the Huascarán National Park and International Biodiversity Reserve. The road along the long axis of the Valley forms one of three principal transect routes over the Cordillera Blanca and reaches a high pass at the Portachuelo de Llanganuco (4,767 m a.s.l.) and it continues down the east side.

At elevations between 3,500 and 4,500 m a.s.l., land cover reflects that of high-altitude grasslands, including the moist Puna (jalca) and páramo (high elevation grass and shrub) ecoregions. Vegetation within the Valley consists of mountain short grass, Polylipis scrub and alpine wastes. Páramo soils are important regulators of headwater hydrology (Harden 2006). Relative humidity is often less than 30%, except when fog is present and during the wet season. Puna plants (Smith and Young 1987; Smith 1988) must have adaptations to resist or avoid desiccation. In addition, the Polylepis sericea, which dominates forest patches in the Valley, allows for supercooling of all its tissues to avoid freezing damage on clear nights (Rada et al., 1996; Goldstein et al., 1994). Plant growth also is cold-limited, so many plants have narrow or

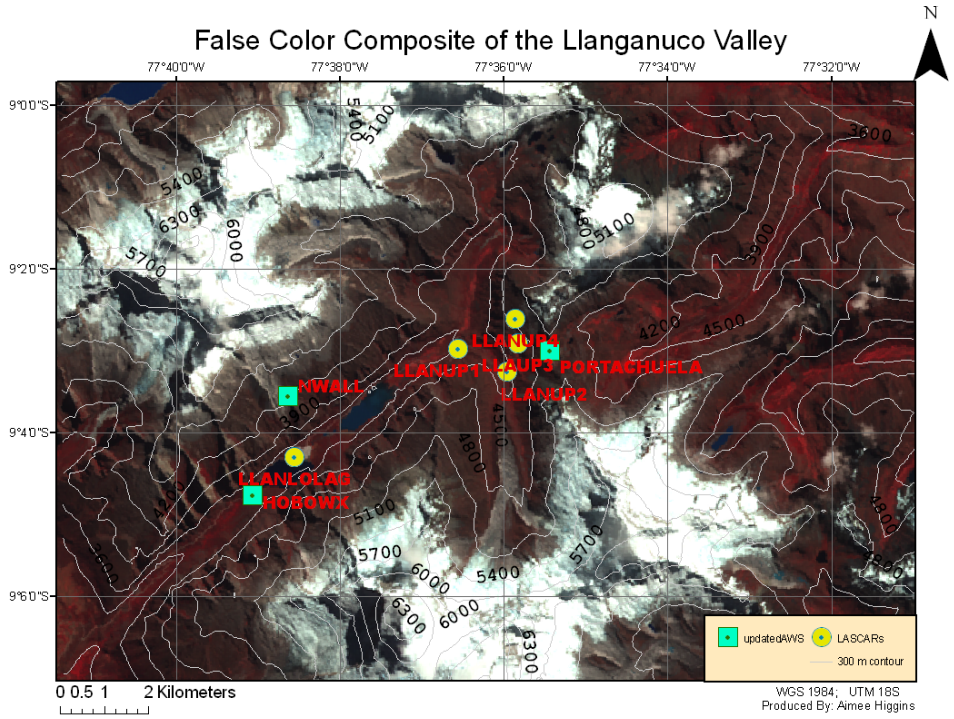

Figure 2. 30 meter resolution LandSat ETM+ false color composite image of the Llanganuco Valley and location of weather instruments: note that glaciers flank the Valley to the north and south of southwest-northeast trending valley. Far eastern and western stations were located outside the valley domain.

small leaves to minimize exposed surface area, and much of the vegetation is near the ground to retain heat.

Rainfall and glacial meltwater from the Llanganuco Valley feeds the Santa River valley watershed which sustains a broad range of agriculture, including wheat, barley, potato, and corn. The valley has two distinct seasons, the wet season and the dry season. The central wet season months are December through February, while the dry season months are June through August.

It is important to consider the seasonal variation solar path. During the wet season, the sun is to the south of the valley, so that the sun is in the south at midday. During the dry season, the sun is to the north of the valley, so that the sun is in the north at midday. The seasons follow the path of the Inter-Tropical Convergence Zone (ITCZ). "Seasonal variations of humidity are governed by the oscillation of the Inter Tropical Convergence Zone which approaches the Cordillera Blanca… between October and April when about 70 to 80% of the annual precipitation [falls]. From May to September… the ITCZ is far north and a trade wind system causes dry conditions" (Kaser et. al., 2001). The dry conditions enhanced by the rain shadow effect downwind of the mountain range. For the Llanganuco Valley, average total precipitation ranges from 8 (□ = 14) mm for June, July and August of the dry period to 258 (□ = 101) mm for December, January and February of the wet period based on the 1953-1998 monthly totals near the lower lake (Dr. Bryan Mark, personal communication).

Objectives

This project has three primary goals: 1) install an ESN to measure and record meteorological conditions during the dry and wet periods for one annual cycle within the Llanganuco Valley, 2) measure ET at a central location, 3) use LandSat ETM+ images to estimate land cover distribution within the Valley, 4) estimate variability of ET using the Penman-Monteith FAO-56 model, and 5) compare wind and temperature measurements from the ESN with synoptic flow and temperature profiles from NCEP/NCAR Reanalysis gridded data.

METHODS

Embedded Sensor Network: AWS Units

In July 2004, we installed an automatic weather station (AWS, www.onsetcomp.com/ HOBO®) in the Llanganuco tributary valley, HOBOWX (3,850 m a.s.l., Figure 3). The AWS recorded hourly values of wind speed (m s^{-1}), solar radiation (W m^{-2}), wind direction (°), soil temperature (°C) and soil moisture (m^3 m^{-3}). In July 2006, we installed two additional HOBO AWS units, one atop the knee of the south-facing wall, NWall, and the other at the top of the valley, Portachuela (4,750 m a.s.l.). AWS units (Figure 3b) recorded hourly averages of 10-second samples of soil moisture and temperature (at 0.1 and 0.5 m), air temperature, wind speed and direction, relative humidity, and incoming solar radiation. In addition, an automatic rain gage, set up by an Austrian research team, recorded 15-minute precipitation (mm), which were totaled to hourly intervals (Campbell Scientific, in collaboration with the University of Innsbruck, Austria). We were particularly careful with our data syntheses from the humidity sensors, which produced erroneously high values of greater than 100% for about 10% of the hourly data recorded during the wet season due to saturation conditions during portions of the wet season. Fortunately, the humidity sensors responded favorably by decreasing to realistic value under high insolation and lack of rainfall during the daylight hours. Values greater than 100% were adjusted to 100%, under the assumption that the air was saturated. We anticipate that humidity values may be overestimated by a few percent during the entire wet period.

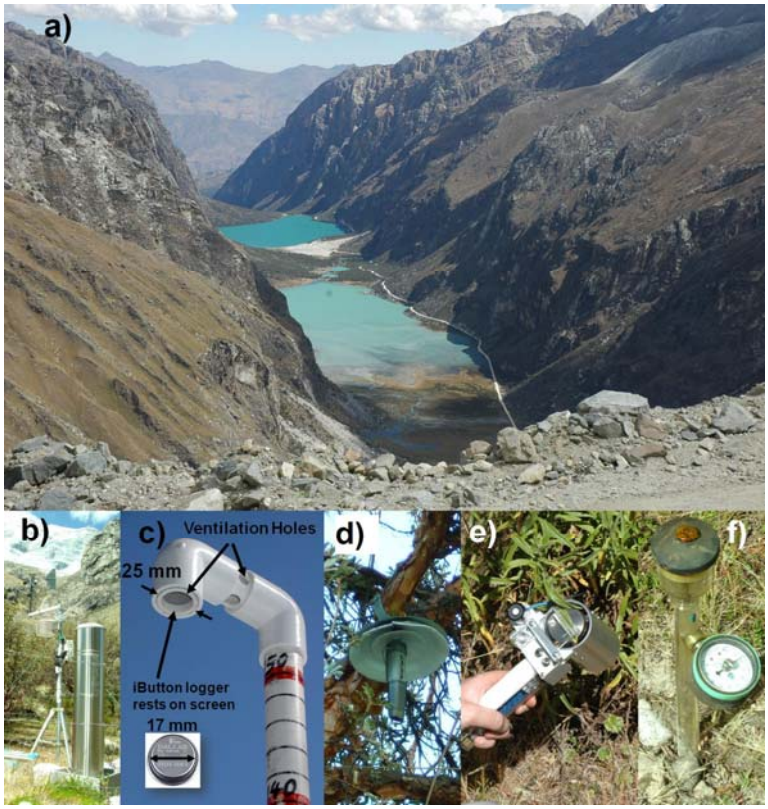

Figure 3. Southwest-looking view of Llanganuco valley from Portachuela site near the highest elevation iButton logger (a) and instrumentation: HOBO AWS and precipitation logger (Kaser, U. Innsbruck) (b), iButton sensor and shield (c), Lascar temperature and humidity logger in tree (d), porometer measuring leaf conductance (e), and tensiometer measuring soil water potential (f). Note the highland grasses, steep rocky walls, terminus of glacier above the north wall, and Santa River valley in the distance.

Embedded Sensor Network: iButton Temperature and Lascar Temperature and Humidity

In June 2005, we installed a set of 8 temperature loggers (iButton Thermochron®) at different elevations ranging from 3,470 to 4,740 m a.s.l., each logger approximately 2 m above the ground (Figure 3c). The advantage to the iButton is its small size and longevity in harsh environments. Each iButton is approximately the size of a nickel, American currency, and is powered by an internal battery and was programmed to record hourly intervals of air temperature. The reported iButton resolution is 0.5°C, accuracy is ±1°C with a range of –40°C to +85°C. Each iButton logger was placed inside a specially designed 2.54 cm inner diameter PVC shield (Figure 3c) that allowed us to embed the sensors in small trees and other shaded inconspicuous locations. The iButton's were exposed to natural ventilation without introducing excessive radiation error, particularly under the extreme insolation common to this environment (Georges and Kaser 2002). One iButton was calibrated under actual field conditions against the naturally ventilated shielded air temperature from the HOBOWX. The calibration from both the wet and dry periods is within the tolerance of the iButton sensor, and the R^2 value was in excess of 0.99 with an offset of less than 0.5 °C, which is within the tolerance of both the iButton and HOBOWX temperature sensors. We expected some impact of radiational warming of the iButtons, particularly during dry season in the afternoon and at one of the higher elevation sites, where shading was less continuous. Approximately every two months, each iButton was checked and the data were downloaded to a laptop computer using the iButton USB port adaptor. The following year, 2006-2007, was used to evaluate the effects of elevation on ET by replacing the iButton network with new sensors that recorded both air temperature and humidity. The network of eight LASCAR USB sensors (Figure 3d), hung by wire in trees at 2 meters above the ground, recorded hourly air temperature (°C) and relative humidity (%); dew point temperature (°C) and vapor pressure (kPa) were calculated for estimating ET (http://www.lascarelectronics.com/). Each LASCAR was shaded by a cone-shaped, gray-painted, tin "hat" with two Styrofoam plates to reduce the impact of radiation heating. Table 1 summarizes the location and elevation of the entire network.

Table 1 Location and time period examined for Llanganuco embedded sensor network. This paper does not include measurements from NWALL

Identification	Sensor/Period	Lon. (deg)	Lat.	Elev. (m a.s.l.)
HOBOWX	AWS/04-07, iButton/05-06, LASCAR/06-07	-77.6512	-9.07943	3,840
LLAN-LOLAG	iButton/05-06, LASCAR/06-07	-77.6427	-9.07162	3,850
LLAN-UPLAG	iButton/05-06, LASCAR/06-07	-77.6214	-9.05375	3,860
LLAN-UP1	iButton/05-06, LASCAR/06-07	-77.6093	-9.04958	3,950
LLAN-UP2	iButton/05-06, LASCAR/06-07	-77.5994	-9.05432	4,140
LLA-UP3	iButton/05-06, LASCAR/06-07	-77.5972	-9.04847	4,350
LLAN-UP4	iButton/05-06, LASCAR/06-07	-77.5977	-9.04355	4,560
PORTACHUELA	iButton/05-06, AWS/06-07, LASCAR/06-07	-77.5906	-9.05000	4,760
NWALL	AWS/06-07, iButton/05-06, LASCAR/06-07	-77.6440	-9.05923	4,540

We compare composite diurnal cycles of meteorological components for wet and dry periods during the 2005 and 2006 seasons. We synthesize all data from the 8 iButton temperature loggers (2005) HOBOWX and the precipitation logger into hourly values to create 24-day periods during the 2005 dry (17 June to 11 July) and wet (7 to 31 December) seasons. The following season, we synthesized data from HOBOWX, NWall, Portachuela and 8 Lascar temperature and humidity loggers for 44-day periods during the dry season (19 July to 31 August 2006) and the wet season (1 January to 13 February 2007). Wind direction was not recorded at NWall. These sample periods were chosen based on data set consistency and proximity to the historically dry and wet seasons. Data were checked for quality and missing or erroneous data were filled through linear interpolation. Vector components of wind speed were calculated to evaluate the variability of the

wind at the HOBOWX and Portachuela sites, as represented by the wind constancy, and to derive valid composite averages of speed and direction. Wind constancy is the mean vector over the mean scalar wind speeds and hence a measure of consistency in wind direction. Mean vector speed is determined by breaking the horizontal wind vector into components, taking the 24-hour averages of each component and recalculating the average vector speed. In the case of humidity sensor saturation during the wet period, records greater than 100%, which occurred for less than 5% of the relative humidity datasets during the wet periods, were adjusted to 100% prior to further analysis and modeling. We created composite averages of 24 hourly measurements for the wet and dry periods—the diurnal cycle. Hence, composites are averages for each hour over the 24-day periods in 2005 and the 44-day periods in 2006 and 2007.

LandSat ETM+ Land Cover

The data used for landcover determination included a 90 meter resolution digital elevation model (DEM) and a 30 meter resolution LandSat ETM+ image (http://landsat.org/). The LandSat ETM+ image was used for vegetation analysis within the valley. The ArcGIS extension, Image Analysis created by Leica Geosystems, was used to derive a Transformed Normalized Difference Vegetation Index (TNDVI) to distinguish land types; $[(\text{Band 4} - \text{Band 3}) \div (\text{Band 4} + \text{Band 3}) + 0.5]^{1/2}$. Band 4 is the near infrared and Band 3 is the visible red wavelength of the electromagnetic spectrum emitted by the surface features. The resulting raster map was used for unsupervised classification. The unsupervised classification created a new raster with classes making it possible to transform the raster into a vector data necessary for ET modeling. The 90-m resolution DEM provided slope values and azimuth and the LandSat image provided a 30-m resolution image for creating the final land cover map with contours. In addition we used the DEM with ArcGIS to estimate potential insolation at the HOBOWX site for dates centered on the dry and wet periods, June and December.

Direct Measurements of ET and Soil Water Potential

In July 2006 we measured two critical surface parameters for calculating ET, including soil water potential and leaf conductance. We measured leaf conductance and transpiration rate with the LI-1600M steady state porometer (Figure 3e) (www.licor.com/), average leaf width and average vegetation height. In addition, we measured soil water potential at dry and moist locations in a 50 m × 50 m area around the HOBOWX site using the 2725 Jet Fill Tensiometer (Figure 3f) (www.soilmoisture.com). Soil water potential controls moisture availability for maintaining vegetation, where low values imply high resistance for root uptake and high values promote root uptake, thus an important component of ET.

Modeling of ET Distribution

The Ref-ET computer model, developed at the University of Idaho (Allen, 2000), was used to model reference ET, ET_0. This program estimates reference ET with an option to use any of fifteen common theoretical equations currently applied throughout the United States and Europe. The calculations require hourly or daily weather data measurements made available by the user (University of Idaho, 2002). This project incorporates the widely accepted FAO-56 algorithm of the Ref-ET model. Hourly values of air temperature, relative humidity, solar radiation, wind speed, and precipitation served as input for the Ref-ET model. Ref-ET's FAO-56 method was applied for dry and wet season data at the HOBOWX and Portachuela sites. All sites measured temperature and relative humidity. Solar radiation, wind speed and precipitation, were interpolated for the remaining six sites, all located at elevations between the Portachuela and HOBOWX sites. Actual ET samples for different vegetation types around the HOBO site were taken at noon time in the dry season using a porometer that measures leaf transpiration directly (Hellström and Mark, 2006). Because of lack of rainfall, soil evaporation is negligible during the dry season, so ET is primarily transpiration. The samples were divided into the four different vegetation types based on height. Lichen was < 0.1 m, grass cover was <0.1 m to 0.5 m, shrubs were between 0.6 m to 2.0 m and trees were over 2.0 m. ET values were averaged within their group and compared against the Ref-ET model result for the HOBOWX location.

NCAR-NCEP Reanalysis

We postulated that strong afternoon heating would create up-valley breeze that opposes the prevailing easterly synoptic flow pattern above the valley. Upper air data available through the National Center for Environmental Predictions (NCEP-DEO AMIP-II Reanalysis, 2002) provided a synoptic overview of temperature, winds, relative humidity and Geopotential height. In particular, we extracted U (west-east) and V (south-north) component wind data to compare the synoptic wind vectors to that from the AWS for the composite dry and wet seasons (NCEP Reanalysis 2 data provided by the NOAA/OAR/ESRL PSD, Boulder, Colorado, USA, from their web site at http://www.esrl.noaa.gov/psd/). Data were downloaded and analyzed for the 500 hPa (mb) level, geopotential height contours of 5840 to 5870 m a.s.l., to represent the free atmosphere over the Llanganuco valley. We expected this comparison to show that the valley wind system is decoupled from the synoptic flow during times of strong solar heating, hence the valley creates a thermally-directed flow that would affect ET, as opposed to channeling of synoptic flow.

RESULTS

Embedded Sensor Network (ESN)

We analyzed ESN data from dry and wet seasons for two consecutive annual cycles, 2005 and 2006-2007. We evaluated the meteorological variations at the valley-centered HOBOWX and the temperature profiles from the iButton from the 2005 season and differences between the HOBOWX and Portachuela sites from the 2006-2007 season. We focused on diurnal variations to compare the wet and dry periods, as described below.

Comparison of wet and dry period diurnal cycles (2005)

Inter-comparisons for dry and wet composite diurnal cycles of air temperature, relative humidity, incident solar radiation (insolation), precipitation, wind speed and direction, and iButton temperatures were examined. The new iButton sensor network initiated by this project permitted high resolution, discrete monitoring of air temperature at different elevations within a pro-glacial valley. Table 2 summarizes the meteorological field measurement results during the 2005 season. Figures 4-7 illustrate the diurnal cycles and seasonal differences for the dry and wet periods. It is important to note that meteorological results from this single annual cycle should not be compared to multi-year studies, given the potential for interannual variability in alpine valleys within the Cordillera Blanca, and we make this clear by presenting two full annual cycles of data. The El Niño Southern Oscillation (ENSO), a weak La Niña in 2005 and a weak El Niño in 2006-07 (Figure 4), produced significant microclimate differences within the Llanganuco Valley (Tables 2 and 3). For example, the wet season (summer in Southern Hemisphere) temperature is lower than the dry during the 2005 La Niña and the reverse is true during the 2006-07 El Niño. In addition, the El Nino of 2007 created anomalously high precipitation during the dry season. The impact of ENSO events are not the focus of this paper, but it demonstrates the need for sustained long-term observations to better understand the processes affecting micrometeorological conditions within pro-glacial valleys.

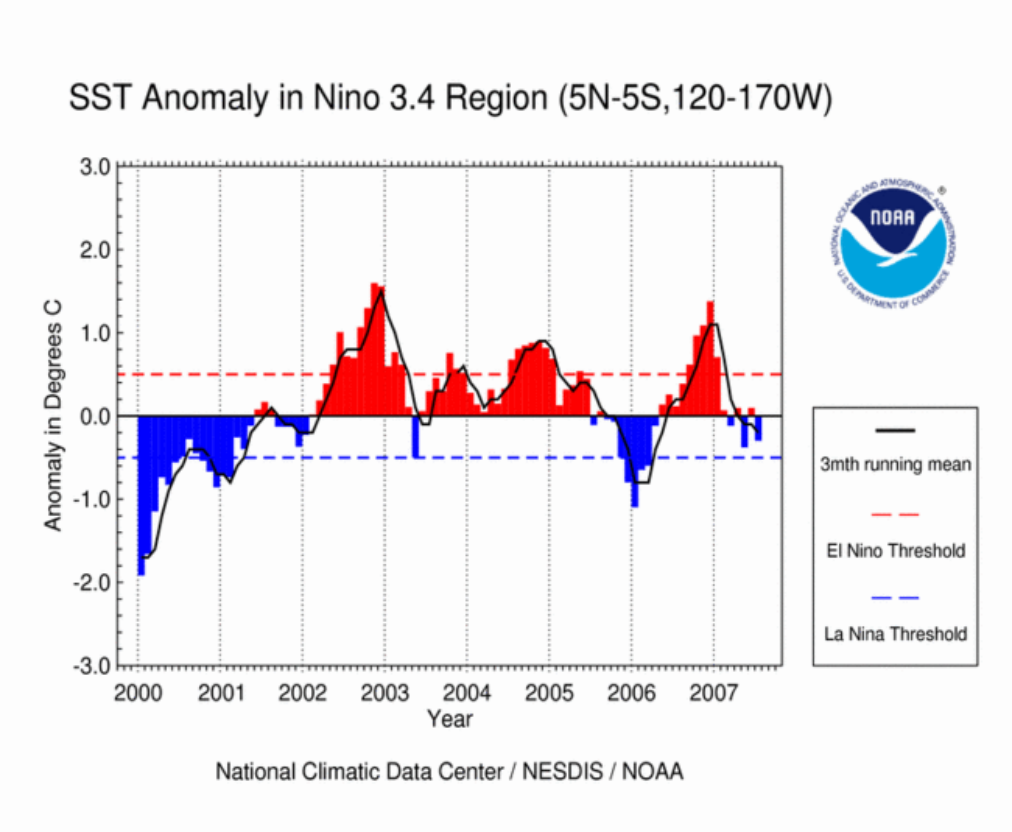

Figure 4. ESNO cycle 2000-2007: NOAA National Climatic Data Center, State of the Climate: El Niño/Southern Oscillation Analysis for July 2007, published online August 2007, retrieved on February 2, 2011 from http://www.ncdc.noaa.gov/sotc/enso/2007/7.

Table 2 2005 La Niña season: Daily average or total of meteorological forcing for composite dry and wet days. Results are shown for the HOBO AWS, left, and the iButton air temperature sensor network, right. The standard deviation is shown in parentheses. The Wet/Dry ratio demonstrates the seasonal difference. Wind constancy is a measure of how variable the hourly wind is throughout the dry and wet period diurnal composites. The last two rows on the right give the average daily lapse rate and extrapolated freezing elevation for the dry and wet periods. Note this is not a true lapse rate, rather the air temperature profile from lower to upper-most part of the long Valley axis. Data for the iButton installed on the east side of the Valley are not shown, as it was not part of the current analysis.

HOBO Weather Station	Dry	Wet	Wet/ Dry		iButton Elevation	Dry	Wet	Wet/ Dry
units below					m	(°C)	(°C)	
Air Temp. (°C)	7.6 (0.8)	6.7 (0.7)	0.87		4760	2.84 (0.80)	1.77 (0.78)	0.62
Max. Temp. (°C)	16.0 (1.2)	12.7 (2.2)	0.79		4560	4.39 (0.80)	3.06 (0.78)	0.70
Min. Temp. (°C)	1.5 (1.2)	3.6 (1.0)	2.40		4350	5.31 (0.82)	3.56 (0.71)	0.67
Temp. Range (°C)	14.5	9.1	0.63		4140	6.68 (0.79)	5.66 (1.79)	0.85
RH (%)	59.5 (12.2)	92.4 (8.3)	1.55		3950	8.12 (0.68)	5.48 (0.94)	0.67
Vapour Pressure (kPa)	0.62 (0.12)	0.90 (0.06)	1.45		3850	7.49 (1.09)	6.24 (0.95)	0.83
VP Deficit (kPa)	0.43 (0.14)	0.08 (0.09)	0.19					
Insolation (MJ m^{-2})	16.8 (1.8)	13.3 (4.9)	0.80		Lapse Rate (°C km^{-1})	6.4 (1.2)	6.5 (0.8)	0.66
Wind (m s^{-1})	1.42 (0.51)	1.18 (0.51)	0.83		0°C Elev. (m)	5210 (225)	4925 (115)	0.95
Wind Direction (°)	39	233	N/A					
Wind Constancy	0.54 (0.26)	0.72 (0.25)	1.33					
–0.10 m Soil Moist. (m^3 m^{-3})	0.005 (0.001)	0.122 (0.063)	26.4					
–0.10 m Soil Temp. (°C)	13.8 (0.8)	12.8 (1.2)	0.93					
Precipitation (mm day^{-1})	0.08 (0.09)	7.36 (8.15)	92.0					

Table 3 2006-2007 El Niño season: Daily average or total of meteorological forcing for composite dry and wet days. Results are shown for HOBOWX, left, and the Lascar air temperature sensor network, right. The standard deviation is shown in parentheses. The Wet/Dry ratio demonstrates the seasonal difference. Wind constancy is a measure of how variable the hourly wind is throughout the dry and wet period diurnal composites. The last two rows on the right give the average daily lapse rate and extrapolated freezing elevation for the dry and wet periods. Note this is not a true lapse rate, rather the air temperature profile from lower to upper-most part of the long Valley axis. Data for the iButton installed on the east side of the Valley are not shown, as it was not part of the current analysis.

HOBO Weather Station	Dry	Wet	Wet/ Dry		Lascar Elevation	Dry	Wet	Wet/ Dry
units below					m	(°C)	(°C)	
Air Temp. (°C)	9.2 ()	9.9 ()	1.08		4760	2.49 ()	3.87 ()	1.56
Max. Temp. (°C)	18.0 ()	17.0 ()	0.94		4560	4.04 ()	5.33 ()	1.31
Min. Temp. (°C)	-0.5 ()	1.0 ()	2.00		4350	4.19 ()	5.18 ()	1.24
Temp. Range (°C)	18.5	16.0	0.86		4140	6.15 ()	7.22 ()	1.17
RH (%)	58.5 ()	83.2 ()	1.41		3950	8.22 ()	8.89 ()	1.08
Vapour Pressure (kPa)	0.65 ()	1.00 ()	1.53		3850	8.09 ()	8.92 ()	1.10
VP Deficit (kPa)	0.60 ()	0.26 ()	0.43					
Insolation (MJ m^{-2})	18.3 ()	13.5 ()	0.74		Lapse Rate (°C km^{-1})	5.8 ()	5.3 ()	0.88
Wind (m s^{-1})	missing ()	missing ()	N/A		0°C Elev. (m)	5160 ()	5420 ()	1.05
Wind Direction (°)	missing	missing	N/A					
Wind Constancy	missing	missing	N/A					
–0.10 m Soil Moist. (m^3 m^{-3})	0.005 ()	0.122 ()	24.4					
–0.10 m Soil Temp. (°C)	13.8 ()	12.8 ()	0.93					
Precipitation (mm day^{-1})	0.42 ()	3.06 ()	7.3					

Comparison of wet and dry period diurnal cycles (2005)

There are marked contrasts in all variables between wet and dry seasons (Table 2), as shown by the mean and standard deviations of day-to-day variations. The average day during the wet period is 1°C cooler than the dry period (Figure 5a), given greater insolation during the dry period (Figure 5c) and lack of rainfall (Figure 5d) at this particular location. This is contrary to the 1°C higher wet period temperatures derived from multi-year records in nearby locations, e.g. Mark and Seltzer (2005) and Juen et al., (2007), although Juen (2006) states that the monthly mean air temperature from station Querococha are very doubtful. As maximum temperatures dominate, some of this bias toward higher dry period temperature may be attributed to abundant daylight solar heating and the tendency for enhancement from the steep valley walls.

In addition, preliminary data from the 2006 season (not shown herein) suggest that the wet period is about 1°C warmer than the dry, in agreement with longer-term studies. In the present 2005 dataset, we attribute the lower diurnal temperature range of 9.1°C during the wet period, as compared to 14.1°C during the dry period, to increased nocturnal cloud cover presumed likely given persistent precipitation, and evaporative cooling partially offsetting strong insolation during daylight hours (Figure 5c). Vapour pressure ranged from 0.62 kPa during the dry to 0.90 kPa for the wet period (Figure 5e). The VPD of 0.43 kPa for the dry period and 0.08 kPa for the wet period (Figure 5f), suggests far greater potential for ET during the dry period with higher ET under daylight conditions during both periods. Soil temperature (Figure 5g) follows the typical diurnal cycle with about twice the amplitude during the dry season with peak of 18°C during the wet and 25°C during the dry seasons between 1400 and 1600 (UTC-5hrs). Actual ET is largely negated by lack of soil moisture 0.005 m^3 m^{-3} for the dry and 0.122 m^3 m^{-3} for the wet periods (Figure 5h). Despite these first order differences in moisture and related parameters, there is only a 19% reduction in solar irradiance during the cloudier wet period.

Microclimate variability and steep terrain are known to create local circulations (valley and slope winds; Whiteman 1990; Whiteman 2000) and our observations suggest a dominant valley wind system with significant seasonal differences. Several theories attempt to attribute a cause to valley winds ranging from Vergeiner (1987) who emphasizes the importance of horizontal pressure differences to Rampanelli et al., (2004) who modeled subsidence heating in the valley core. We observe distinct seasonal contrasts in both near-surface wind speed and direction (Figures 6a, b). Southwest winds, directed up the Valley during daylight hours of the wet season are consistent with strong insolation (Figure 5c) before noon into the late afternoon. Daytime winds were cross Valley from the west-northwest during the dry period, possibly the result of cold air draining from off the north wall, which receives less direct insolation as the solar disk azimuth is north of the Valley axis. After sunset during the dry period, consistent down-valley winds are probably caused by nocturnal cold air drainage under cloudless skies, but also likely from cross-valley synoptic flow and a curvature-induced secondary circulation (see Weigel and Rotach 2004, Figure 11, page 2,618). On the other hand, nocturnal down slope winds are insignificant during the wet period as clouds enhance downward infrared radiation, as indicated by higher minimum temperature (Table 2) than the dry period (Figures 6c, d).

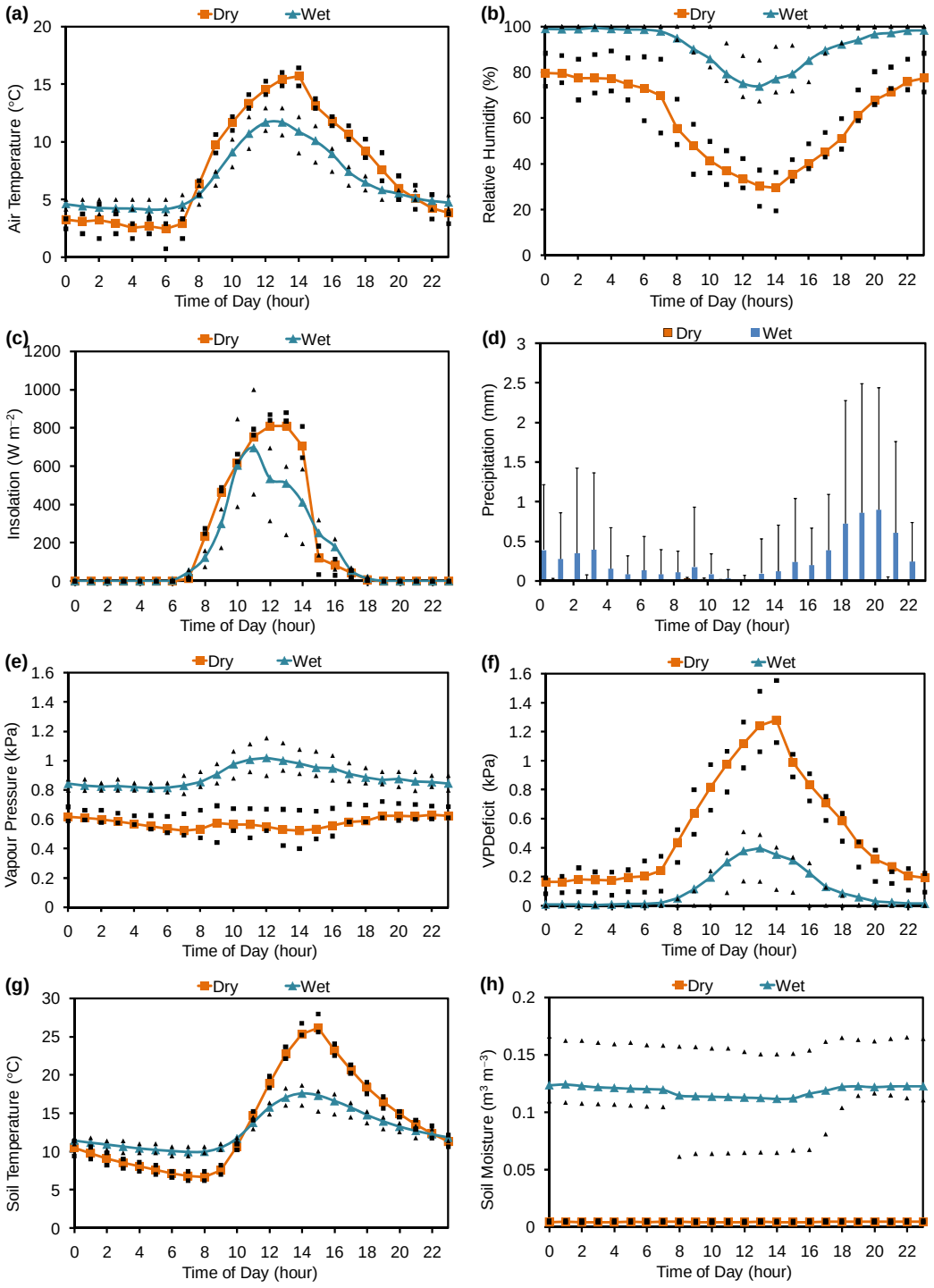

Figure 5. (2005) Depicted are composite diurnal cycles as recorded by the AWS at the base of the lower lake. Comparisons for the dry and wet periods include: air temperature (a), relative humidity (b), incoming global solar radiation (c), hourly total precipitation—note dry is negligible (d), vapour pressure (e), vapour pressure deficit (f), and soil temperature (g) and volumetric water content (h) at a depth of 10 cm. Day-to-day variation is shown by the 1st and 3rd quartiles (25th and 75th percentile) and is designated by small symbols above or below the mean. Time is UTC-5hrs.

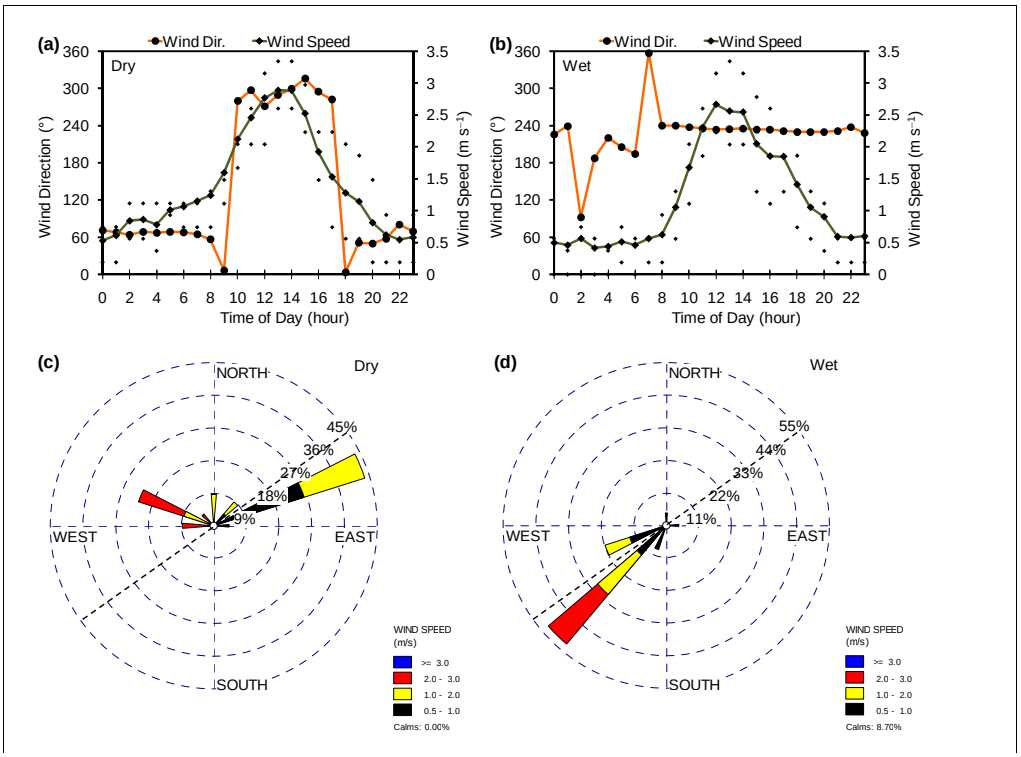

Figure 6. (2005) Composite diurnal cycle of wind vector components as recorded from the AWS: speed with 1st and 3rd quartile showing day-to-day variation and direction for dry (a) and wet (b) periods, and the wind roses for dry (c) and wet (d) periods. The dashed line indicates the compass orientation of the long valley axis. Time is UTC-5hrs.

Figures 7a, b show the strong correlation between air temperature and wind speed for both dry and wet periods for the 24 hours of the composite, which demonstrates, particularly during the wet period, the connection between persistent up-valley winds and warmer near-surface temperature within the Valley. The strong correlation also indicates the strong diurnal tendency of both temperature and wind speed, which suggests that both are strongly related to insolation. The slope of the positive wind speed vs. air temperature relation doubles from the dry to the wet periods, indicative of lower temperature range during the wet period. In an attempt to minimize the impact of diurnal insolation, Figures 7c, d suggests a much weaker correlation when considering the 24 day-to-day variations at 1200, although the correlation remains stronger for the wet period. The warmer winds flow up-valley as shown for the wet period in Figure 6d.

Figures 8a, b show the dramatic diurnal cycle of near-surface temperature profiles, as measured by the iButtons at different elevations, particularly evident during the less cloudy dry season. The composite suggests a slightly steeper temperature profile during the wet period and that the freezing (0°C) elevation is projected to be 4,930 m for the wet and 5,280 m for the dry periods (Figures 8c, d). The observed seasonal cycle of freezing elevation suggests greater potential for glacial recession during the dry season, although this is based only on one annual cycle. In fact, results from continued observations in 2006 (next section, Figure) suggest the opposite trend, with the freezing line at 5,340 m a.s.l. during the wet period and 5,080 m a.s.l. during the dry period. On the other hand, the wind direction during the dry period (Figure 6c) does not promote the direct up-valley winds dominating the wet period (Figure 6d), rather the stronger wind flow from the west and northwest, off the north wall of the Valley. Hence, at least in the composite, wind observations suggest little or no warm air advection between the AWS site and higher elevations. Our analysis of meteorological measurements points to the need for better representation of diurnal cycles of valley winds and interactions with high insolation during both periods and evening peak of precipitation during the evening during the wet period.

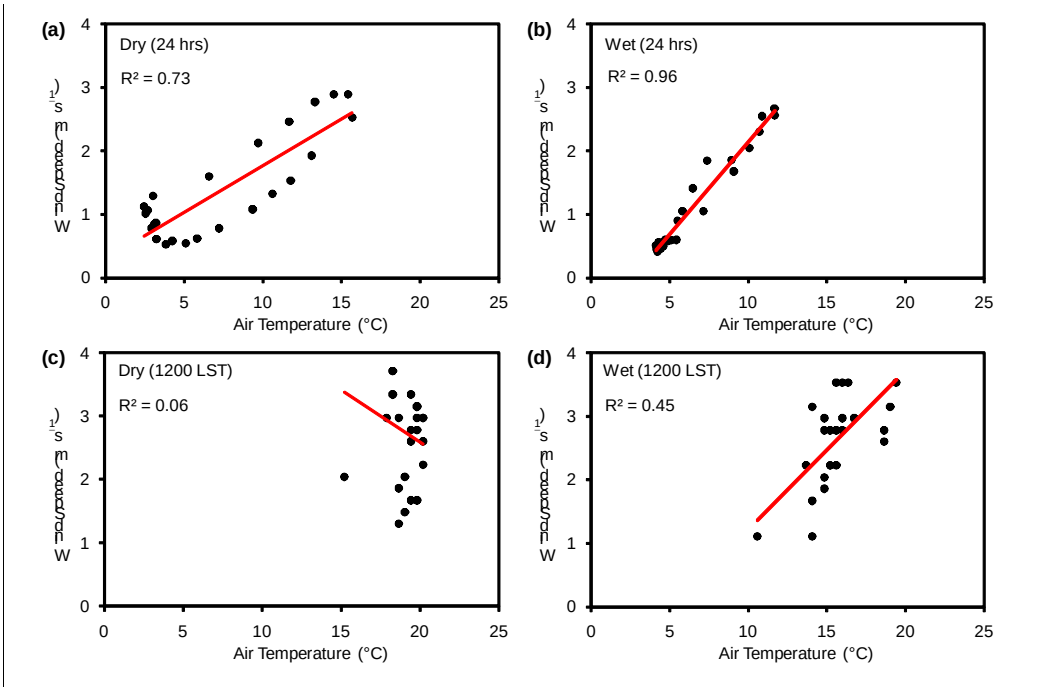

Figure 7. (2005) Composite wind speed versus air temperature for dry (a) and wet (b) periods for 24 hours. Day-to-day wind speed versus air temperature for dry (c) and wet (d) periods for 1200 LST to remove effect of diurnal insolation cycle. The linear regression equation provides a relation between wind speed and air temperature for both seasons and the coefficient of determination (R^2) suggests strong interdependence.

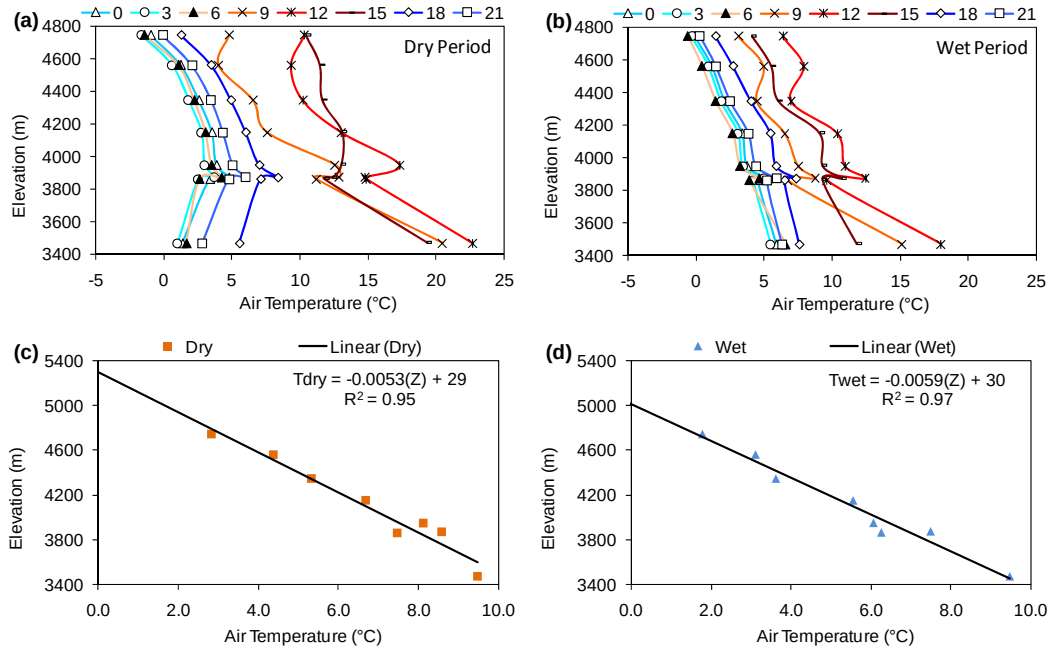

Figure 8. (2005) The near surface air temperature profile from iButton temperature sensor network is shown at three hourly intervals for the composite dry (a) and wet (b) periods. Inversions are positive slopes. The average daily temperature profile (near surface lapse rate) for the dry (c) and wet (d) periods extrapolated to indicate the estimated elevation above which the temperature is below freezing; we iButtons evenly spaced at about 200 m elevation to determine lapse rates.

Comparison of low and high elevation sites for the wet and dry period diurnal cycles (2006-2007)

Of the eight sites, the highest, Portachuela (Port), and lowest, HOBOWX, locations were analyzed to compare the diurnal pattern of weather conditions during the dry and wet periods of 2006-2007. Precipitation (Figure 9a,b) is heavy during the wet season and nearly absent during the dry season. During the dry season, the Portachuela site experiences the most rainfall as compared to the lower HOBOWX site. The HOBOWX site receives little rainfall during the dry season, receiving the least during the midday hours. During the wet season, the HOBOWX site receives the majority of its precipitation during the early nightfall hours, between 1700 and 2000. Another peak of rainfall is seen between 2000 and 2300 (UTC-5hrs). The Portacheula site receives a large amount of its rainfall during the periods 900-1200 and 2100-2300, largely due to topographic enhancement. In general, precipitation occurs in the late afternoon and evening within the central part of the Llanganuco Valley and morning and evening in upper portions.

Solar radiation (Figure 9c) is affected by cloud cover often accompanied by late afternoon daylight precipitation events during the wet season. One would expect that the solar radiation would be more intense during the summer months of December-February. However, the wet season increases the probability of cloud cover, especially in the afternoon. At the HOBOWX location, there is a notable drop in solar radiation between 1000 and 1100, which we attribute to cloud cover, since valley geometry does not promote shading at this time.

Wind speed (Figure 9d) does not vary between the seasons as much as it does throughout the day. The HOBOWX site has the most variance in wind speed during the day. Wind remains calm during the night and peaks at midday. Wind speed is more uniform at Portachuela, and it is the windier of the two locations, largely because of its exposure to the free atmosphere as the highest elevation of all sites along the valley axis.

Temperature cycles (Figure 9e) from coldest at night to warmest around midday at both sites and during both seasons. It is colder at night during the dry season at both sites and cooler during the day at the HOBOWX site. At Portachuela the midday temperatures are about the same for both seasons. The Portachuela site, because of its higher elevation, is the coldest of all sites on average.

Vapor pressure (Figure 9f) reaches higher values during the wet season, which tends to reduce evaporation. During both seasons, the HOBOWX site experiences the higher vapor pressure values compared the Portachuela site. Throughout the valley, the higher elevations experience the lower vapor pressures with a weak correlation to air temperature for both seasons.

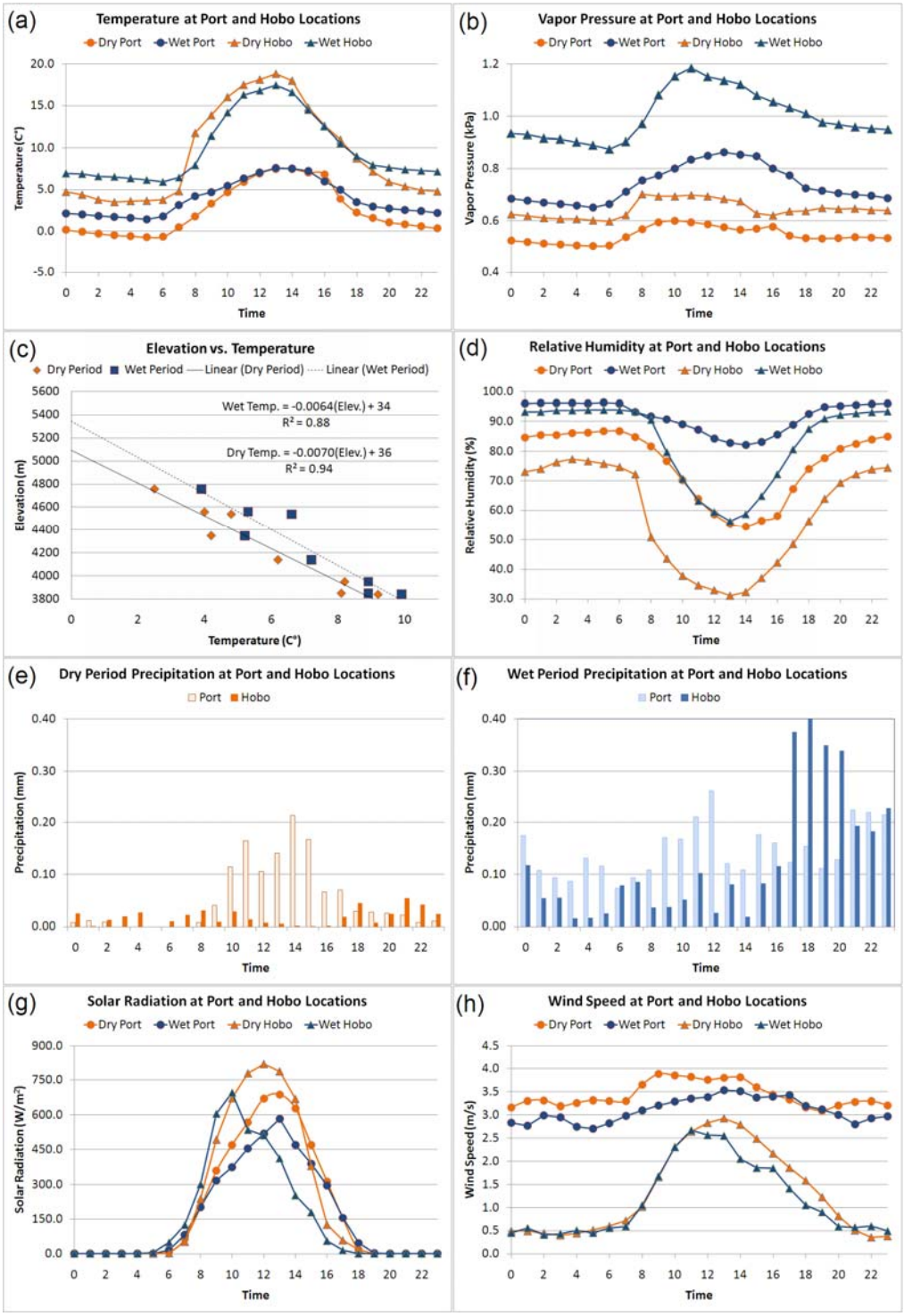

Figure 9. (2006-2007) Depicted are composite diurnal cycles as recorded by the AWS at the base of the lower lake. Comparisons for the dry and wet periods include: air temperature (a), relative humidity (b), incoming global solar radiation (c), hourly total precipitation—note dry is negligible (d), vapour pressure (e), vapour pressure deficit (f), and soil temperature (g) and volumetric water content (h) at a depth of 10 cm. Day-to-day variation is shown by the 1st and 3rd quartiles (25th and 75th percentile) and is designated by small symbols above or below the mean. Time is UTC-5hrs.

LandSat ETM+ Land Cover and Terrain

The classes on the vegetation map created by TNDVI analysis include water and ice, exposed rock, lichen (ground cover less than 0.1 m tall), grass cover, shrub cover and tree cover (Figure 10). GIS and remote sensing combined to create results for a large part of the project. The TNDVI analysis suggests that vegetation covers 52% of the area of the valley, hence the majority of the valley. Vegetation cover ranges from 4% for lichen to 21% for Polylepis trees.

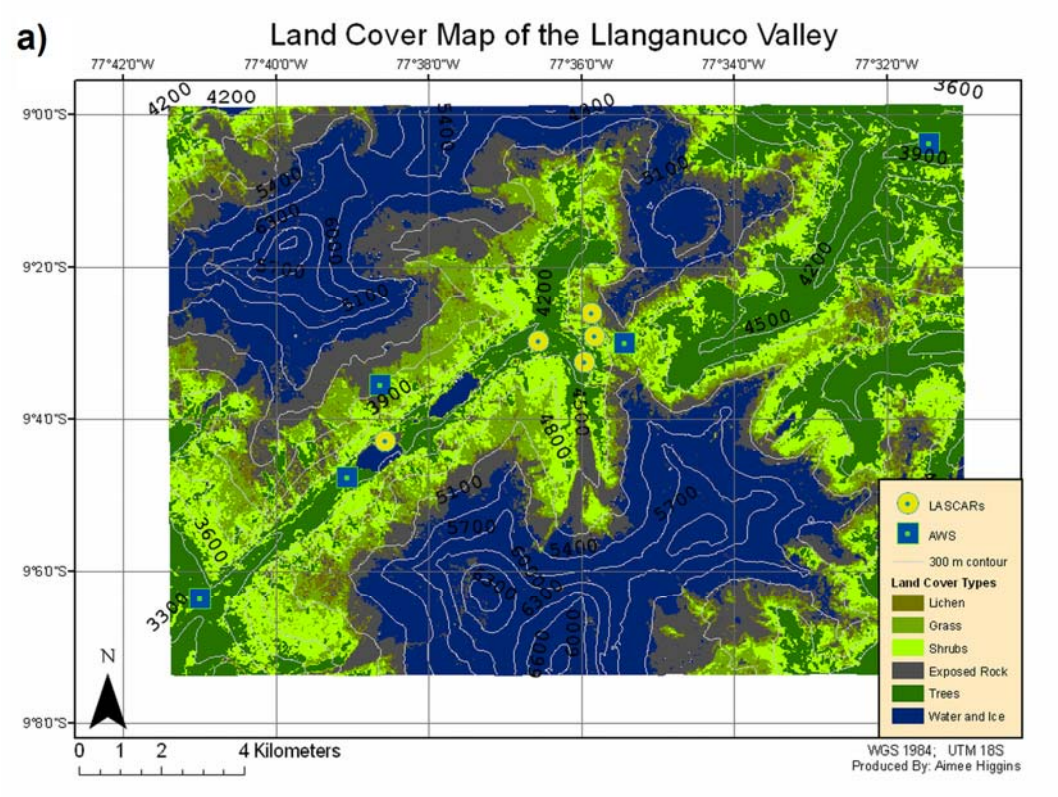

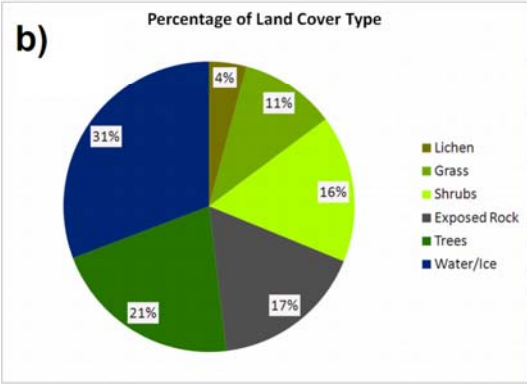

Land Cover Type	Square KM
Lichen	11
Grass	28
Shrubs	43.1
Exposed Rock	44.6
Trees	55.6
Water/Ice	81.1

Figure 10. These figures show the various types of land cover within the valley; note the two meltwater lakes between the two glaciated peaks. Vegetation is confined to subalpine areas below 5100 m (a). The most abundant land cover type is vegetation, lichen, grass, shrubs and trees, which makes up 52% of the valley (b). These groups of vegetation were use to model ET.

Figure 11 shows the high variation in terrain as shown by surface slopes derived from the 90 m DEM.

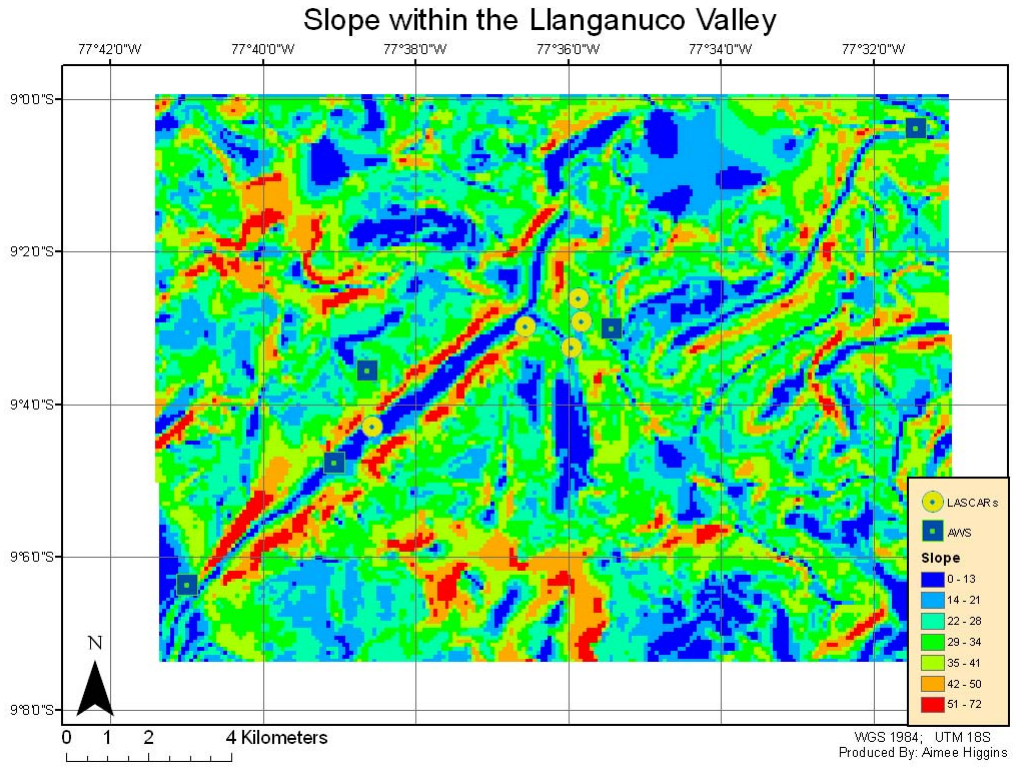

Figure 11. Slope variance within the valley. A slope of 0° would indicate a level surface, while a slope of 90° would indicate that the surface is going vertical. The sensors are in relatively low sloped areas, with slopes between 0-34°. Note the far west and east sensors were not used in this study.

Modeling of ET Distribution

Estimating ET was an important objective of this project. The diurnal cycle of ET (Figure 12 a,b) is strongly driven by insolation. The time of maximum ET is different for the seasons, peaking from 1200 to 1300 during the dry period and from 1000 at higher elevations to 1400 at lower elevations during the wet period, largely a result of migrating cloud cover from lower portions in the valley to upper portions from 1000 to 1400. When comparing all eight sites from 2006-2007 against elevation, it is noted that ET decreases with elevation (Figure 12c) and that this trend is more pronounced with stronger correlation during the dry season. ET also has a diurnal cycle at all eight sites during both seasons. There is a negative correlation between elevation and temperature during both seasons (Figure 12d). It is colder at sites with higher elevations compared to the lower elevations. Extrapolating to the freezing point of water, 0°C, suggests that the freezing elevation is 5100 m during the dry and 5350 m during the wet seasons. The higher freezing line during the wet season would promote enhanced glacial melt above that of the dry season. The HOBOWX site was the only site with in-situ ET measurements taken at noon during the dry period.

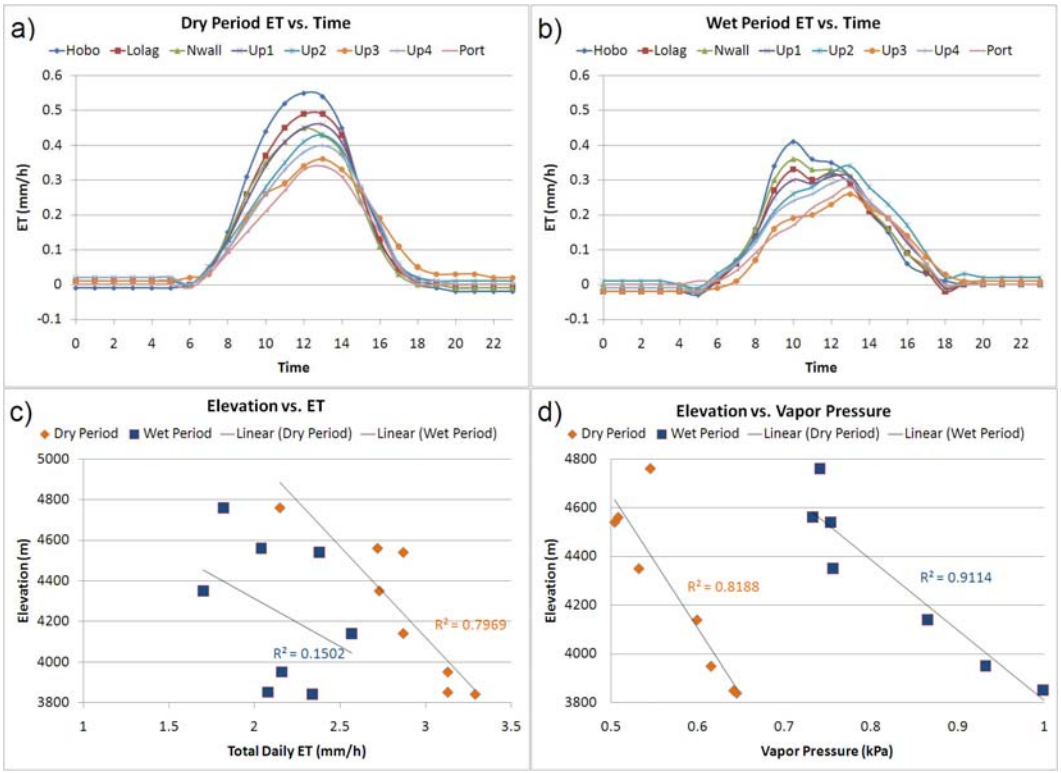

Figure 12. (2006-2007) These figures show the various types of land cover within the valley; note the two meltwater lakes between the two glaciated peaks. Vegetation is confined to subalpine areas below 5100 m (a). The most abundant land cover type is vegetation, lichen, grass, shrubs and trees, which makes up 52% of the valley (b). These groups of vegetation were use to model ET.

During the dry season, lichen produces the most ET per unit area while the trees have the least (Fig. 12a). All these values were higher than the Ref-ET model measurement. However, when you compare the volume of ET between the Ref-ET measurement of 0.55 mm hr^{-1} and the actual ET results, there is no significant difference (Figs. 12 c&d). Trees are responsible for the most volume of ET and lichen is responsible for the least volume of ET.

There is a unique relation between slope, elevation, land cover type and ET. It appears that sites in the 0°-13° sloped areas (Fig. 11) have higher amounts of vegetation types (Fig. 10) that favor higher ET, the trees. Locations with higher slopes, like the North Wall, slopes ranging from 22°-28°, have higher amounts of vegetation which produce less ET, the lichen. In addition to low slopes, the areas with vegetation types that have higher rates of ET are typically at lower elevations. The Hobo site, Lanlolag site, Up1 site and Up2 site have elevations between 3840 m – 4140 m (Figs. 10, 11). These sites predominantly have tree cover as the main type of vegetation. Lichen cover appears to have a factor of elevation and slope. Portachuela is in a relatively low sloped location, between 0°-13° and predominantly has lichen for its vegetation type (Figs. 10, 11). It is also the highest site within the valley, at 4760 m. Up4 and the North Wall site both have an elevation of 4540 m. Up4 is in the 29°-34° slope area and is lichen is the predominant vegetation type. The North Wall site has a slope of 22°-28°, and like Up4, lichen is the predominant vegetation type. Up2 has a low elevation of 4140 m, and a high slope of 29°-34° and has tree cover as the main vegetation type. This shows that elevation has more of an impact on land cover than slope. However, slope does seem to have somewhat of an impact. This research demonstrates what Konzelmann et. al. (1997) found in their research – that vegetation as well as

terrain do factor into ET in an alpine region and that these variables should be "considered more carefully for model calculations of the ET in high mountain areas" (Konzelmann et. al., 1997).

ET was modeled using the Penman-Monteith FAO 56 method. During the dry season actual measurements were taken that could be used to compare to the modeled results. All vegetation types that had actual measurements had higher ET rates compared to the model (Fig. 12b). Despite the model underestimating ET in the alpine valley, it is still an indicator that using this method would work in future research. Konzelmann et. al (1997) also found that "The values of actual ET favorably correlate with those computed with Penman's formulation" (Konzelmann et al., 1997). Garcia et. al. (2004) also found that actual measurements of ET in a Bolivian highland were comparable to modeled results using the Penman method. Garcia et. al. (2004) found that the Penman-Monteith method is "able to account for the effects of the high elevation (high solar radiation but low radiation term) and of the moderate aridity reflected in the vapour pressure deficit, temperature and wind" (Garcia et. al. 2004).

Valley and Synoptic Winds (2005)

Wind roses show the differences in wind speed and direction within the four time periods that we selected which were: 00Z (1900), 06Z (0100), 12Z (0700) and 18Z (1300). The time period that is of particular interest to this study is 18Z because it is the only time period observed during the day. Daytime weather systems are the most unstable systems throughout the day as shown in figures 5a-d. Figure 3 is an illustration of the daily cycle of winds in a mountain terrain (Whiteman, 2000).

Figure 5a is a wind rose from data gathered from HOBOAWS during the dry season. Most of the strong winds during this period come from the northeast, while some of the lighter winds come from the southwest. This suggests that most of the time, wind from the bottom of the valley is blowing upslope and toward the glaciers. Valley winds are either caused by thermally induced pressure gradients with higher pressure at lower elevations or by synoptic scale flow channeling, either forced or pressure-driven (Whiteman, 2000). With an increase in surface temperature due to global climate change, melting of glaciers could be enhanced by locally-forced valley winds advecting warmer air to the summit. NCEP winds (Figure 13b) oppose the HOBOAWS winds (Figure 13a) in general. Strong winds from the northeast would bring cool air from the summit, and channel it down the valley.

Figures 13c and 13d demonstrate strong afternoon valley winds during the wet season. The AWS winds from the southwest oppose the northeast prevalence for the same time from the NCEP reanalysis. But with the data collected from NCEP, winds coming from the northeast would cause glacial expansion. The combination of NCEP and AWS data suggest that surface warming and up-valley winds are not the result of forced channeling and thus may be induce local warm air advection and plausibly promote glacial loss at higher elevations by sensible heat flux. Further work is needed to better understand the energetic of the complex boundary layer formed by the warmer and deeper well-mixed layer created by up-valley and the interaction with shallower katabatic downward flow.

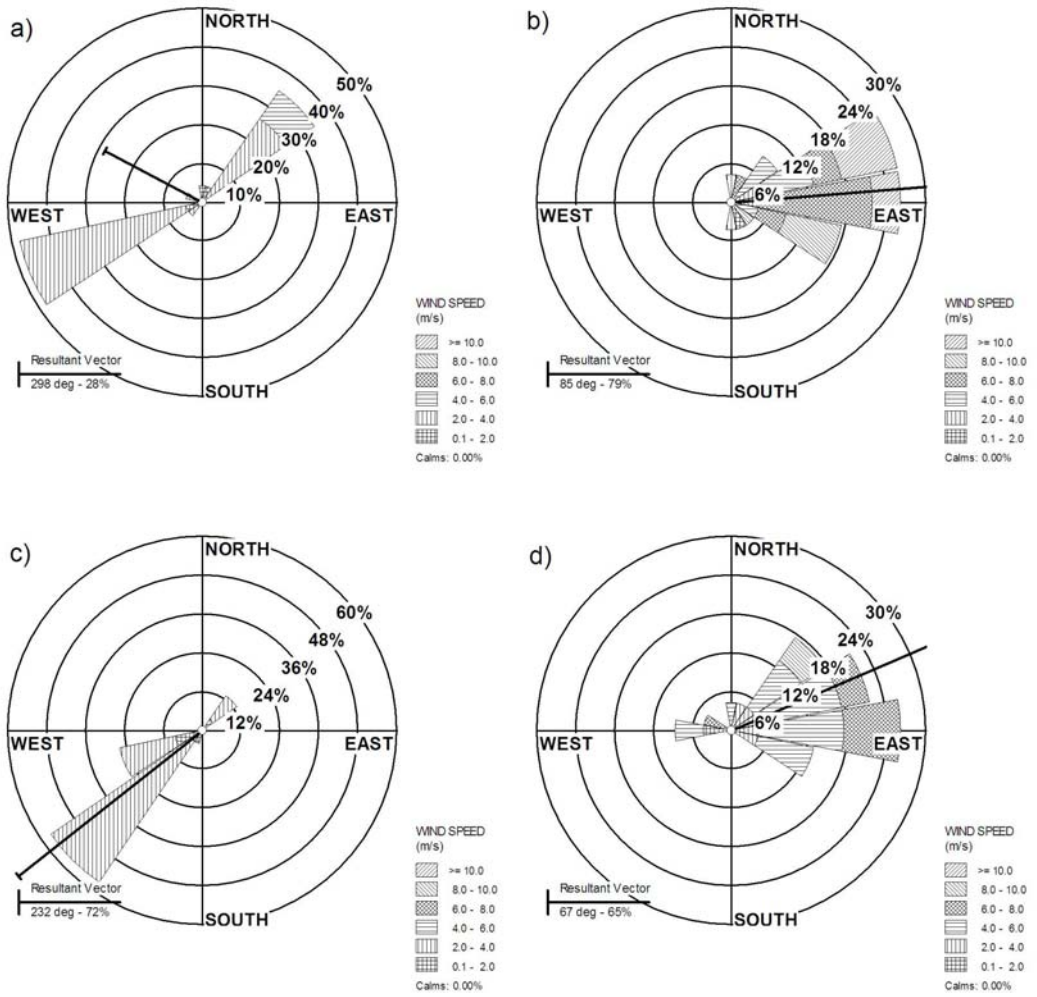

Figure 13. a)18Z Dry AWS. b) 18Z Dry NCEP. c) 18Z Wet AWS. d) 18Z Wet NCEP

The results demonstrate that there is a decoupling between the regional (synoptic) and local scale valley wind systems, particularly during the wet season during periods of strong solar afternoon surface heating. There are many valleys located in the Cordillera Blanca to which this data could be applied. Every valley seems to have its own microclimate, so concluding that what data was found here is found at every valley in the Cordillera Blanca is illadvised but some of the same principles apply, therefore melting in these areas may be occurring for the same reasons.

ACKNOWLEDGEMENTS

Funding for this project was provided by The Ohio State University, Department of Geography and Office of International Affairs. Additional support was provided by the Presidential Fellows Award, and two undergraduate research awards through the Adrian Tinsley Program at Bridgewater State University. Thanks to Delphis Levia at the University of Delaware for loaning the porometer for field measurments. We are grateful for the collaboration with Peruvian Institute of Natural Resources (INRENA), especially the timely collection and transmission of data by Jesús Gómez, INRENA-Huaraz, Perú.

REFERENCES[2]

Allen RG (2000) Using the FAO-56 dual crop coefficient method over an irrigated region as part of an evapotranspiration intercomparison study. J Hydrol (Amst) **229**:27–41

Allen RG, Pruitt WO, Wright JL, Howell TA, Ventura F, Snyder R, et al (2006) A recommendation on standardized surface resistance for hourly calculation of reference ET0 by the FAO56 Penman–Monteith method. Agric Water Manage **81**:1–22

Bendix J, Rollenbeck R, Reudenbach C (2006) Diurnal patterns of rainfall in a tropical Andean valley of southern Ecuador as seen by a vertically pointing K-band Doppler radar. Int J Climatol **26**:829–846

Berengena J, Gavilán P (2005) Reference evapotranspiration estimation in a highly advective semiarid environment. J Irrig Drain Eng **131**:147–163

Bowman KP, Collier JC, North GR, Wu Q, Ha E, Hardin J (2005) Diurnal cycle of tropical precipitation in Tropical Rainfall Measuring Mission (TRMM) satellite and ocean buoy rain gauge data. J Geophys Res 110:D21104, doi:10.1029/2005JD005763

Byon JY, Lim GH (2005) Diurnal variation of tropical convection during TOGA COARE IOP. Adv Atmos Sci **22**:685–702

Bradley RS, Vuille M, Diaz HF, Vergara W (2006) Threats to water supplies in the tropical Andes. Science **312**:1755–1756

Canqui E (1993) Determinación de la evapotranspiración potencial por lisimetr'ıa en la estación experimental de Patacamaya. Thesis. Technical University of Oruro, Bolivia:85 pp

Chen SS, Houze RA (1997) Diurnal variation and life-cycle of deep convective systems over the tropical Pacific warm pool. Q J R Meteorol Soc **123**:357–388

Dai A (2001) Global precipitation and thunderstorm frequencies. Part II: Diurnal variations. J Clim **14**:1112–1128

Duvel JP, Kandel RS (1985) Regional-scale diurnal variations of outgoing infrared radiation observed by METEOSAT. J Clim Appl Meteorol **24**:335–349

Egger J, et al (2005) Diurnal circulation of the Bolivian Altiplano, Part I: Observations. Mon Weather Rev **133**:911–924

Eichinger WE, Cooper DI (2007) Using lidar remote sensing for spatially resolved measurements of evaporation and other meteorological parameters. Agron J **99**:255–271

Federer CA, Vörösmarty C, Fekete B (2003) Sensitivity of annual evaporation to soil and root properties in two models of contrasting complexity. J Hydromet **4**:1276–1290

Francou B, Ribstein P, Saravia R, Tiriau E (1995) Monthly balance and water discharge of an inter-tropical glacier: Zongo Glacier, Cordillera Real, Bolivia, 16S. J Glaciol **41**:61-67

Francou B, Vuille M, Wagnon P, Mendoza J, Sicart JE (2003) Tropical climate change recorded by a glacier in the central Andes during the last decades of the twentieth century: Chacaltaya, Bolivia, 16 degrees S. J Geophys Res-Atmos 108(D5): 4154. doi:10.1029/2002JD002959

Garcia M (2001) Evapotranspiración de referencia en el Altiplano Boliviano. Reporte presentado al Programa Nacional de Riego. BID-PRONAR, Bolivia:120 pp

Garcia M, Raes D, Allen R, Herbas C (2004) Dynamics of reference evapotranspiration in the Bolivian highlands (Altiplano). Agric Forest Meteorol **125**:67–82

Garreaud RD, Wallace JM (1997) The diurnal march of convective cloudiness over the Americas. Mon Wea Rev **125**:3157–3171

Georges C, Kaser G (2002) Ventilated and unventilated air temperature measurements for glacier-climate studies on a tropical high mountain site. J Geophys Res-Atmos **107**:4775–4787

Goldstein G, Meinzer FC, Rada F (1994) Environmental biology of a tropical treeline species Polylepis sericea. Tropical Alp Environ: Plant form and function, ed. Rundel PW, Smith AP, Meinzer FC Cambridge: University Press:129–150

Gray WM, Jacobson RW (1977) Diurnal variation of deep cumulus convection. Mon Wea Rev **105**:1171–1188

Hardy DR, Vuille M, Braun C, Keimig F, Bradley RS (1998) Annual and daily meteorological cycles at high altitude on a tropical mountain. Bull Amer Meteor Soc **79**:1899–1913

[2] There are some unused references in the list.

Harden CP (2006) Human impacts on headwater fluvial systems in the northern and central Andes. Geomorph **79**:249–253
Juen I (2006) Glacier mass balance and runoff in the tropical Cordillera Blanca, Perú. Dissertation. Tropical Glaciology Group, Institute of Geography, Innsbruck, Austria
Juen I, Kaser G, Georges C (2007) Modelling observed and future runoff from a glacierized tropical catchment (Cordillera Blanca, Perú). Global Plan Change **59**:37–48
Kaser G, Juen I, Georges C, Gomez J, Tamayo W (2003) The impact of glaciers on the runoff and the reconstruction of mass balance history from hydrological data in the tropical Cordillera Blanca, Peru. J Hydrol **282**:130–144
Kite GW, Droogers P (2000) Comparing evapotranspiration estimates from satellites, hydrological models and field data. J Hydrol **209**:3–18
Konzelmann, T., P. Calcana, G. Müller, L. Menzel., and H. Lang (1997) Energy Balance and Evapotranspiration in a High Mountain Area during Summer. J. App. Meteor. **36**: 966-973.
Mapes BE, Warner TT, Xu M, Negri AJ (2003) Diurnal patterns of rainfall in northwestern South America. Part I: Observations and context. Mon Wea Rev **131**:799–812
Mark BG, Seltzer GO (2003) Tropical glacier meltwater contribution to stream discharge: a case study in the Cordillera Blanca, Peru. J Glaciol **49**:271-281
Mark BG, Seltzer GO (2005) Recent glacial recession in the Cordillera Blanca, Peru (AD 1962-1999). Quat Sci Rev **24**:2265–2280
McNulty BA, Farber DL, Wallace GS, Lopez R, Palacios O (1998) Role of plate kinematics and plate-slip-vector partitioning in continental magmatic arcs: Evidence from the Cordillera Blanca, Peru. Geol **26**:827–830
NCEP-DEO AMIP-II Reanalysis (R-2) (2002) M. Kanamitsu, W. Ebisuzaki, J. Woollen, S-K Yang, J.J. Hnilo, M. Fiorino, and G. L. Potter. Bul Atmos Met Soc:1631-1643
Nesbitt SW, Zipser EJ (2003) The diurnal cycle of rainfall and convective intensity according to three years of TRMM measurements. J. Clim **16**:1456–1475
Paço TA, Ferreira MI, Conceic¸ao N (2006) Peach orchard evapotranspiration in a sandy soil: comparison between eddy covariance measurements and estimates by the FAO 56 approach. Agric Wat Manage **85**:305–313
Paredes RD (1995) Determinación de la evapotranspiración potencial (ETP) en lis´ımetros de drenaje simple. Thesis. Technical University of Oruro, Bolivia:110 pp
Penman HL (1948) Natural evaporation from open water, bare soil and grass. Proc. Roy. Soc. London. **193**:120–146
Penman HL (1963) Vegetation and hydrology. Tech. Comm. No. 53. Commonwealth bureau of soils, Harpenden, England 125 pp
Poveda G, Mesa OJ, Salazar LF, Arias PA, Moreno HA, Vieira SC, Agudelo PA, Toro VG, Alvarez JF (2005) The diurnal cycle of precipitation in the tropical Andes of Colombia. Mon Wea Rev **133**: 228–240
Rada F, Azocar A, Briceno B, Gonzalez J, García-Nuñez C (1996) Carbon and water balance in Polylepis sericea, a tropical treeline species. Tree **10**:218–222
Ramirez E, Francou B, Ribstein P, Descloitres M, Guerin R, et al (2001) Small glaciers disappearing in the tropical Andes: a case-study in Bolivia: Glaciar Chacaltaya (16 degrees S). J Glaciol **47**:187–194
Rampanellie G, Zardi D, Rotunno R (2004) Mechanisms of up-valley winds. J Atmos Sci **61**: 3097–3111
Rotach MW, Andretta M, Calanca P, Weigel AP, Weiss A (2008) Turbulence characteristics and exchange mechanisms in highly complex terrain, Acta Geophysicae **56** (1):194–219
Rucker M, Banta RM, Steyn DG (2008) Along-valley structure of daytime thermally driven flows in the Wipp Valley. J. Appl. Meteor. Climatol. **47**:733–751
Smith AP, Young TP (1987) Tropical alpine plant ecology. Ann Rev Ecol Syst 18:137–158
Smith DN (1988) Flora and vegetation of the Huascarán National Park, Ancash, Peru, with preliminary taxonomic studies for a manual of the flora. Ph.D. dissertation. Iowa State University, Ames
Sorooshian S, Gao X, Hsu K, Maddox RA, Hong Y, Gupta HV, Imam B (2002) Diurnal Variability of Tropical Rainfall Retrieved from Combined GOES and TRMM Satellite Information. J Climate **15**:983–1001

Steinacker, R (1984) Area-height distribution of a valley and its relation to the valley wind. Contrib Atmos Phys **57**:64–71
Suleiman A, Crago R (2004) Hourly and Daytime Evapotranspiration from Grassland Using Radiometric Surface Temperatures. Agron J **96**:384–390
Tolk JA, Evett SR, Howell TA (2006) Advection Influences on Evapotranspiration of Alfalfa in a Semiarid Climate. Agron J **98**:1646–1654
UNEP (1997) World Atlas of Desertification 2nd Ed. United Nations Environment Programme. Edited by Middleton N, Thomas D. 182 pp. ISBN No: 340691662
Vergara W, Deeb AM, Valencia AM, Bradley RS, Francou B, et al. (2007) Economic Impacts of Rapid Glacier Retreat in the Andes. Eos, Trans, Amer Geophys Union **88**:261–268
Vergeiner I (1987) An elementary valley wind model. Meteorol and Atmo Phys **36**: 255–263
Vuille M, Kaser G, Juen I (2008) Glacier mass balance variability in the Cordillera Blanca, Peru and its relationship with climate and the large-scale circulation. Glob Plan Change **62**:14–28
Vuille M, Bradley RS, Werner M, Keimig F (2003) 20th century climate change in the tropical Andes: Observations and model results. Clim Change **59**:75–99
Wagnon P, Ribstein P, Kaser G, Berton P (1999) Energy balance and runoff seasonality of a Bolivian glacier. Glob Plan Change **22**:49–58
Wagnon P, Ribstein P, Schuler T, Francou B (1998) Flow Separation On Zongo Glacier, Cordillera Real, Bolivia. Hydrol Proc **12**:1911–1926
Weigel AP, Rotach MW (2004) Flow structure and turbulence characteristics of the daytime atmosphere in a steep and narrow Alpine valley. Quart J Roy Meteorol Soc **130**: 2605–2627
Weigel AP, Chow FK, Rotach MW, Street RL, Xue M (2006) High-resolution large-eddy simulations of flow in a steep Alpine valley. Part II: Flow Structure and Heat Budgets, J Appl Meteorol Climatol **45**(1):87–107
Weigel AP, Chow FK, Rotach MW (2007) The effect of mountainous topography on moisture exchange between the "surface" and the free atmosphere. Boundary-Layer Meteorol **125**:227–244
Whiteman CD (1990) Observations of thermally developed wind systems in mountainous terrain. Atmospheric Processes over Complex Terrain, Meteor. Monograph. Amer Meteor Soc **45**: 5–42
Whiteman CD (2000) Mountain Meteorology. Fundamentals and Applications, Oxford University Press, NewYork: 355 pp
Worden J, Noon D, Bowman K, et al. (2007) Importance of rain evaporation and continental convection in the tropical water cycle. Nature **445**:528–532
Yang G-Y, Slingo J (2001) The Diurnal Cycle in the Tropics. Mon Weather Rev **129**:784–801.